

SEDIMENTOLOGY OF THE JEZERO CRATER WESTERN FAN DEPOSIT: 2. SECULAR CHANGES IN THE STYLE OF CHANNELIZATION. T. A. Goudge¹, D. Mohrig¹, B. T. Cardenas¹, C. M. Hughes¹, J. S. Levy², and C. I. Fassett³, ¹Jackson School of Geosciences, The University of Texas at Austin, Austin, TX, ²University of Texas Institute for Geophysics, Austin, TX, ³Dept. of Astronomy, Mount Holyoke College, South Hadley, MA. (Contact: tgoudge@jsg.utexas.edu)

Introduction: The hydrologically open Jezero crater paleolake basin on Mars contains a well-exposed sedimentary fan deposit in its interior (**Fig. 1**). This fan deposit, the westernmost of two within the basin [1], is one of the most convincing examples of a martian delta deposit based on geologic context, morphology, mineralogy, and exposed stratigraphy [1-4]. This delta deposit also contains sedimentary structures interpreted as point bars and inverted channels (**Fig. 2**) that have been exhumed subsequent to construction of the deposit [1,3]. Here we present a detailed analysis of the variable style of channelization, sedimentation, and incision associated with channels of the Jezero crater western delta to help constrain the paleohydraulic and geologic history preserved by this deposit.

Methods: We mapped identifiable channel-related stratigraphy exposed on the upper portion of the deposit surface (**Fig. 1**), which we interpret as the exhumed topset of the delta. Mapping was completed using three high-resolution digital elevation models (DEMs) and corresponding orthorectified images derived from HiRISE images [5] using the NASA Ames Stereo Pipeline (ASP) [6-8].

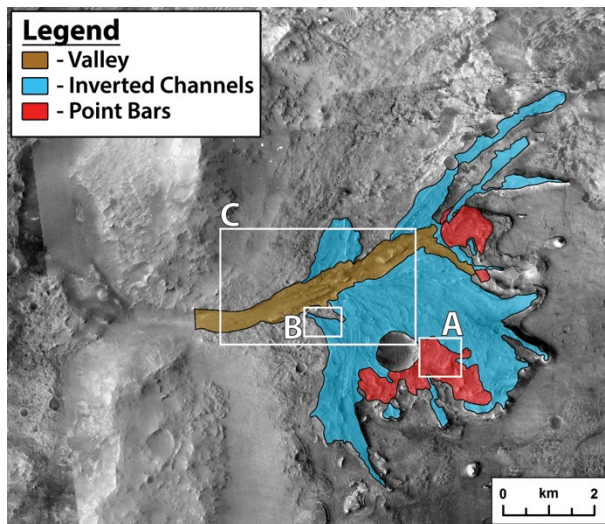


Fig. 1. The Jezero crater western delta deposit showing the three classes of channel-related structures across the delta. White boxes indicate the locations of parts A-C in **Fig. 2**. Mosaic of CTX image D14_032794_1989 and HiRISE images PSP_003798_1985, ESP_037396_1985 and ESP_036618_1985.

Results: We identify three distinct classes of channel-related structures in the Jezero crater western delta

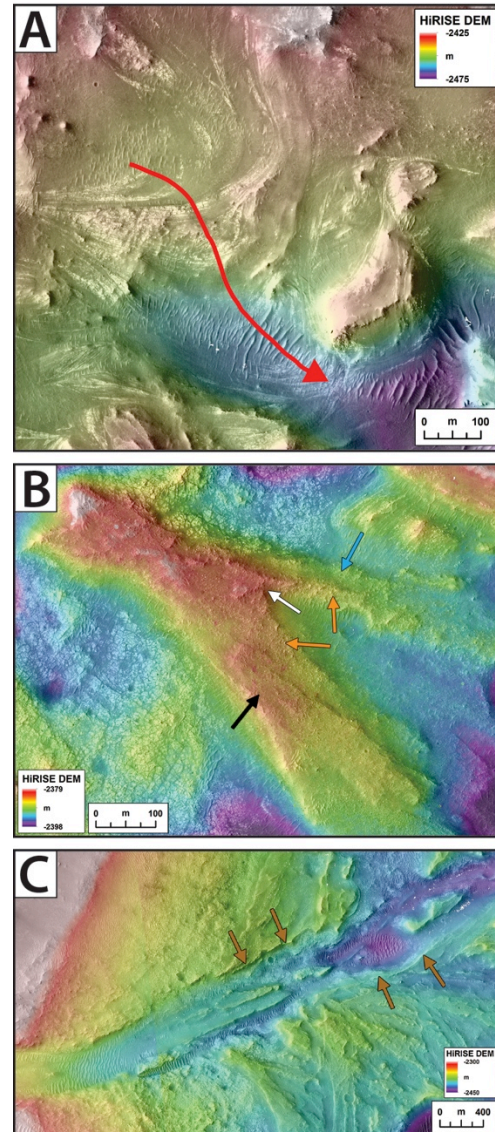


Fig. 2. The three classes of channel-related structures within the western delta deposit. **(A)** Point bar deposited by a meandering channel. Red arrow shows general direction of lateral channel migration. **(B)** Stack of multiple exhumed, inverted channels (arrows; cyan is lowest, orange is middle, and black is highest in stack). White arrow shows possible channel bifurcation. **(C)** Valley (brown arrows) cutting into the delta deposit. **(A)** and **(B)** show HiRISE-derived DEM from images ESP_037396_1985 and ESP_042315_1985 overlain on HiRISE image ESP_037396_1985. **(C)** shows HiRISE-derived DEMs from images ESP_037396_1985 and ESP_042315_1985, and ESP_036618_1985 and ESP_037119_1985 overlain on a mosaic of HiRISE images ESP_037396_1985 and ESP_036618_1985.

deposit (Fig. 1,2). The first class of structure is alternating dark- and light-toned, curved strata that we interpret as eroded point bar deposits (Fig. 2A) [3]. The second class of structure is relatively straight, topographically high deposits that we interpret as inverted channel bodies (Fig. 2B) [1,3]. The inverted channels show multiple, stacked deposits, as well as potential evidence for channel bifurcation, where a single inverted channel splits into two channel bodies at the same stratigraphic level (Fig. 2B, white arrow). The final class of structure is not depositional, but rather is a valley that cuts down into the fan deposit (Fig. 2C).

The three classes of channel-related structures have systematic differences in their horizontal (Fig. 1) and stratigraphic (Fig. 3) position. The point bar deposits are the stratigraphically lowest and are primarily observed in erosional windows through the overlying inverted channels, which make up the majority of the exhumed delta topset. The valley, on the other hand, is cut into the inverted channel deposits, and is the stratigraphically highest channel-related structure we observe.

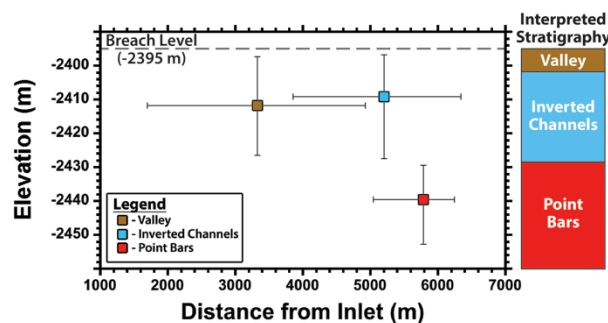


Fig. 3. Plot showing the relative position of the three main classes of channel-related structures, along with a schematic showing the interpreted stratigraphy. Plot points show the median value, and error bars show range from 25th to 75th percentile of the data. Although the valley is at a lower median elevation than the inverted channels, it is stratigraphically higher, as the former cuts into the latter. Horizontal dashed line indicates the elevation of the outlet breach [1].

Discussion: We interpret the three classes of channel-related structures as indicative of three periods of channel development during unique phases in the evolution of the Jezero crater paleolake.

The stratigraphically lowest point bar deposits (Fig. 2A) are indicative of meandering channels. Point bars form from the accumulation of sediment on the inner bank of channel bends, and are associated with lateral migration and deformation of the channel itself [9,10] (Fig. 2A, red arrow). Lateral migration rates and point bar growth in coastal rivers tend to decrease towards the shoreline due to hydraulic influences that control sediment transport in the backwater zone [11,12]. Therefore, we suggest that the point bar deposits formed during an early phase of fluvial activity when the lake shoreline

was further from the site of deposition, towards the basin center.

We interpret the higher, stacked inverted channel deposits (Fig. 2B) as sediment deposited on the floors of channels during aggradation of the delta. These channel bodies are relatively straight with minimal evidence for lateral migration, and the stacking of multiple inverted channel bodies suggests the routing of these channels was influenced by subtle topographic signatures left by older, under-filled channels. Additionally, we identify several locations that appear to show channel bifurcations (Fig. 2B, white arrow), which are common features in channel networks of terrestrial deltas [13,14]. We hypothesize that the inverted channels were deposited once the Jezero crater basin filled to a stable lake level controlled by a breach point.

We interpret the valley (Fig. 2C) as a fluvial erosional feature that has cut into the delta deposit. Incision of the previously deposited delta topset sediment implies a drop in lake level, and we hypothesize that this valley formed during the waning stages of lacustrine activity in the Jezero crater paleolake.

Future Work: Ongoing work involves collection of a variety of morphometric data from each of the three channel-related structures. For the point bar deposits, we plan to fit three dimensional curved surfaces to each of the layers mapped within the deposit to determine the radius of curvature of the meander, and how this varied as the bend migrated and deformed. Additionally, the total thickness of a single set of strata interpreted to represent one point bar (e.g., Fig. 2A) provides a rough proxy for channel depth. For the inverted channel deposits, we plan to collect width and slope values. Finally, for the valley, we will collect width and depth measurements along the valley length. All of these values will help to constrain the paleohydraulics of the flow associated with each of the three classes of channel-related structures described here. These data will allow us to further reconstruct the history of fluvio-lacustrine activity within the Jezero crater paleolake basin, and how this relates to the broader picture of early martian climatic evolution.

References: [1] Fassett, C., J. Head (2005), *GRL*, **32**:L14201. [2] Ehlmann, B., et al. (2008), *Nat. Geosci.*, **1**:355–358. [3] Schon, S., et al. (2012), *PSS*, **67**:28–45. [4] Goudge, T., et al. (2016), *this meeting*, #1122. [5] McEwen, A., et al. (2007), *JGR*, **112**:E05S02. [6] Broxton, M., L. Edwards (2008), *LPSC 39*, #2419. [7] Moratto, Z., et al. (2010), *LPSC 41*, #2364. [8] Beyer, R., et al. (2014), *LPSC 45*, #2902. [9] Ikeda, S., et al. (1981), *J. Fluid Mech.*, **112**:363–377. [10] Parker, G., et al. (2011), *Earth Surf. Process. Landforms*, **36**:70–86. [11] Hudson, P., R. Kesel (2000), *Geology*, **28**:531–534. [12] Nittrouer, J., et al. (2012), *GSA Bull.*, **124**:400–414. [13] Edmonds, D., R. Slingerland (2007), *JGR*, **112**:F02034. [14] Edmonds, D., R. Slingerland (2008), *Water Res. Research*, **44**:W09426.